

Single Deformation Occurrence During Testing of Kenaf Composite Through Momentum Trapping Modification on Split Hopkinson Pressure Bar

Muhammad Fauzinizam Razali, Sareh Aiman Hilmi Abu Seman*, Mohd Syakirin Rusdi and Siti Nuha Majiddah Abdul Aziz

School of Mechanical Engineering, Universiti Sains Malaysia, 14300 Nibong Tebal, Pulau Pinang, Malaysia

ABSTRACT

In dynamic applications, the effective use of kenaf composite materials necessitates comprehensive and precise elucidation of their mechanical response under high strain rate loading conditions. Accurately measuring the sample's deformation can only be achieved using a pulse-trapping technique. In this study, a dynamic momentum trapping mechanism that is simple to assemble and configure was constructed and affixed to a conventional Split Hopkinson Pressure Bar (SHPB) system. The effectiveness of the verified momentum trap approach was shown when the secondary wave of compression was decreased by 50 percent in the application of momentum trapping that stopped the specimen from coming in contact with the incident bar, resulting in a much-improved correlation between various strain rates and the failure of kenaf composite microstructure.

Keywords: Failure correlation, momentum trapping, Split Hopkinson pressure bar, strain rates

ARTICLE INFO

Article history:

Received: 08 September 2023

Accepted: 18 January 2024

Published: 25 July 2024

DOI: <https://doi.org/10.47836/pjst.32.4.14>

E-mail addresses:

mefauzinizam@usm.my (Muhammad Fauzinizam Razali)

sarehaiman@usm.my* (Sareh Aiman Hilmi Abu Seman)

syakirin@usm.my (Mohd Syakirin Rusdi)

nuha.abdulaziz99@gmail.com (Siti Nuha Majiddah Abdul Aziz)

* Corresponding author

INTRODUCTION

Based on its strong mechanical properties, low density, excellent properties of damping and biodegradability, kenaf fiber reinforced composite has attracted a great deal of interest (Mansingh et al., 2022). It has been documented that kenaf composite has a high cellulose content (70.4wt%), contributing to its high strength (Millogo et al., 2015). Even so, the kenaf fiber showed good mechanical properties, thermal stability and a strong

fiber-matrix adhesion compared to other natural fibers (Alshammari et al., 2023; Arjmandi et al., 2021). The kenaf composite has recently been used increasingly for automotive secondary structural parts (Uzoma et al., 2023; Wazeer et al., 2023). For example, Toyota Boshoku Corp. has used kenaf composite as the interior components of its newly developed electric concept car, Toyota LQ (Vasilash, 2020), while its European division, Lexus, has applied kenaf composite as package shelves (Holbery & Houston, 2006). Another leading car maker, General Motors, has also used kenaf composite in Saturn L300s and Opel Vectra's as packaging trays and door panel inserts (Holbery & Houston, 2006). In addition, a study made by Arockia Dhanraj et al. (2019) on kenaf composites' mechanical properties has also approved its suitability for automotive structural applications such as front modules, door panels and bumper beams.

In order to design components or structures built of kenaf composites, one needs to have a comprehensive grasp of the mechanisms of dynamic deformation and failure, particularly in the event of impact loading events like car collisions. Hence, to improve the design for structural components better suited to this specific application in the automotive sector, it is particularly necessary to characterize kenaf composite under loading conditions that are close to those experienced in real life (Abidin et al., 2023; Tamrakar et al., 2021).

Kenaf composite has been widely investigated for its mechanical response either at quasi-static (Bhambure et al., 2023; Ochi, 2008; Saba et al., 2015) or at dynamic loading rates (Bhambure et al., 2023; Omar et al., 2010). The relationship between loading rates, the mechanical properties and the type of failure observed macroscopically (Omar et al., 2010) and microscopically (Seman et al., 2019b; Sharba et al., 2016) has been found in several studies. However, the kenaf composite is not reportedly interrupted during dynamic loading, where specimens are only individually loaded (Omar et al., 2010). At higher stress rates, a lack of interrupted tests can lead to an inaccurate relationship between various stress rate levels and failure in the microstructure.

The standard Hopkinson pressure bar (SHPB) configuration should usually not be used for disrupted tests as stress wave reflections from the free ends reload the specimen several times (Omar et al., 2010; Zhang et al., 2020). Nemat-Nasser et al. (1991) first eliminated reflected stress waves by using a momentum trap technique applied to two different split Hopkinson pressure bars working in compressive and tensile directions. The momentum trap in a compressive SHPB consisted of transfer flanges, an incident tube, and a rigid mass, all with the same impedance as the input bar and was co-axial to it. Using SHPB, Song and Chen (2004) recorded another set-up for interrupted compressive dynamic testing conducted on soft materials. The momentum trap in these configurations consisted only of a transfer flange and a large rigid mass passed through the input bar. Therefore, the reaction mass was compensated for by a small gap that had accuracy regulated by a collar located at the free end of the input bar. A tandem momentum trap has been developed by Prot

and Cloete (2016) to avoid the effort of adjusting the gap between the rigid mass and the flange. This design, which can provide a single specimen loading event, comprises a pair of concentric tubes that are impedance matched, co-axially aligned with, and configured to function sequentially with the input bar.

The methods above included the rigid mass or second momentum trap to create a returning tensile wave when it was impacted by the incident tube or flange. However, attaching a huge rigid mass to the existing SHPB setup might be complicated as it would affect the movement of the incident bar if it were not properly installed. On top of that, even though a tandem momentum trap developed by Prot and Cloete (2016) did not need a precision gap, implementation of this technique is quite complicated as different diameters of momentum traps and bushing were needed in this design. Thus, a simple dynamic testing technique was developed in this research, based on a momentum trap concept, to provide an exact correlation between different stress rate levels and microstructural damages to a kenaf composite. The technique was based on Nemat Nasser 's work, but different working theories, designs and dimensions of the momentum trap components were used to fit the current SHPB. The method of the energy trap modified for the Split Hopkinson Pressure Bar was examined in depth. Data from several dynamic recovery experiments performed on kenaf composites and high-speed images are presented to demonstrate the validity of the hypothesis.

METHODOLOGY

Split Hopkinson Pressure Bar

The kenaf composite was dynamically characterized by a compression SHPB (Figure 1) available in Universiti Sains Malaysia. Key elements of the setup included bearings and a

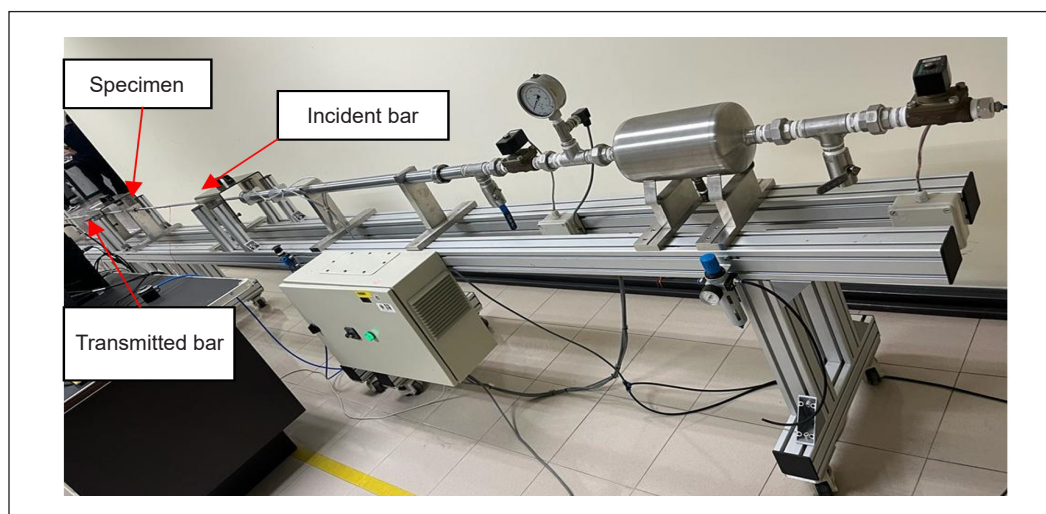


Figure 1. Split Hopkinson pressure bar

sturdy support system for the input bar, the output bar, and the striker bar to keep the three bars in uniaxial alignment under the intense impact of a pressurized nitrogen gas gun with a power of up to 70 psi. All bars are 12 mm in diameter but different in length, where input and output bars are 1500 mm long, whereas the striker bar is 152 mm long. In addition, to avoid superimposing the incident and reflected pulses, the ratio of length to diameter of 20 of the input and output bars was required. The bars had a density of 8000 kg/m³, Young’s modulus of 200 GPa, and a bar wave velocity of 5000 m/s; they were crafted from high-carbon chromium alloy steel.

Momentum Trapping Design

Components of the momentum trap were made from high-strength steel tubing, with inner tube diameters chosen to match those of the incident bar and outer tube diameters processed so that the tubes’ cross-sectional areas meet the impedance requirement. The length of the momentum traps has been selected to be as long as the striker so that the strain gauges mounted to the middle are not interfered with. Finally, the 60 mm long flange was also made of high-strength steel, which can achieve strength and rigidity while maintaining a low mass. The momentum trap and Split Hopkinson Pressure Bar (SHPB) specification are given in Table 1.

Table 1
SHPB and momentum trap component specifications

	Input bar	Output bar	Striker	Rigid mass	Incident tube	
Material	High carbon chromium alloy steel	High carbon chromium alloy steel	High carbon chromium alloy steel	High strength steel	High strength steel	High strength steel
Length (mm)	1500	1500	152	152	152	25
Inner diameter (mm)	–	–	–	12	12	12
Outside diameter (mm)	12	12	12	24	24	24
Impedance (kPa.s/m)	13,941	13,941	13,941	13,941	13,941	13,941
Density (kg/m³)	8000	8000	8000	7800	7800	7800

As shown in Figure 2, the momentum trapping device includes a flange attached as a momentum trap to the end of the incident bar, an incident tube and a rigid mass through which the incident bar passes. The rigid mass was attached at a fixed position to prevent any movement. The momentum trap parts are arranged concentrically with the incident bar and aligned with each other. The stress waves are transmitted through a flange fixed on the incident bar between the momentum trap pieces.

The gap between the incident bar and the rigid mass had been established. This default gap has been correctly managed so that if the secondary loading wave reflected

in the incident bar emerges, the incident bar will unexpectedly stop due to the reversed compressive pulse impact from the incident tube. Since the excessive momentum is trapped to ensure a single load on the sample, the condition of the specimen under the identified load is well established, and the development of damage inside the specimen is easier to interpret.

The working mechanism of a modified SHPB is shown in Figure 2. In the first stage, the activation of the gas gun resulted in a collision between the striker and the flange connected to the input bar. This phenomenon gives rise to two separate compression waves, with the first wave propagating through the incident bar and the subsequent wave propagating through the tube (Figure 3a). Following the collision, the striker will experience little rebound due to encountering an impedance lower than the combined impedance of the incident bar and flange (Figure 3a).

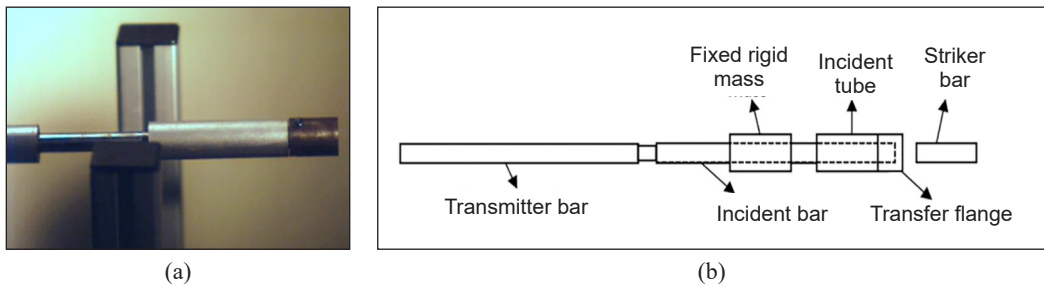


Figure 2. (a) Implementation of a momentum trapping on a SHPB; and (b) Schematic illustration of momentum trapping on a SHPB

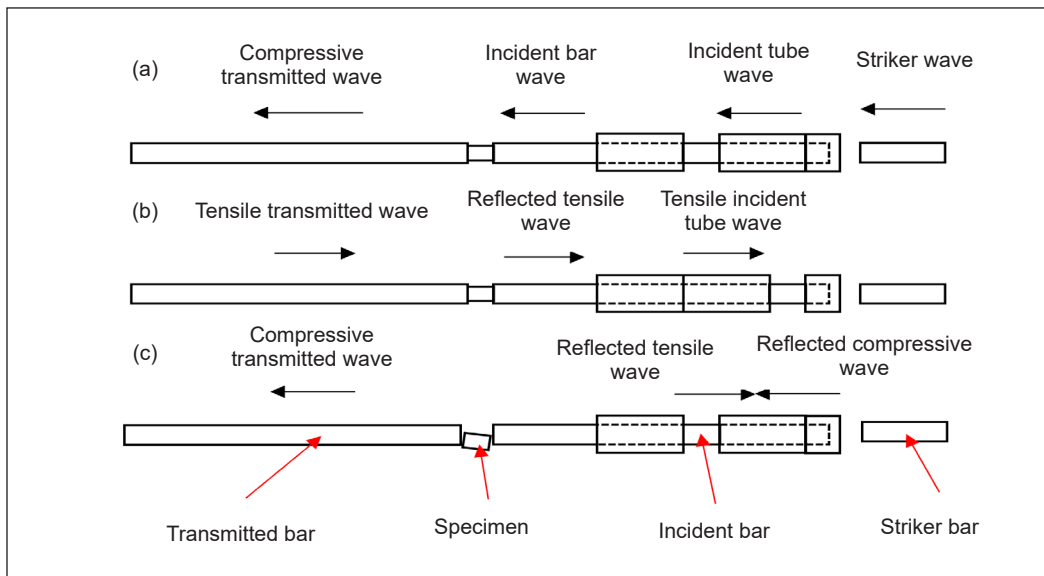


Figure 3. Schematic illustration of the operating principle of a standard SHPB with a momentum trap

Due to the matched impedance of all components comprising the momentum trap and the input bar, the second wave is transmitted to the rigid mass without reflection. Upon the arrival of the compressive wave at the unfixed end of the immovable rigid mass, it underwent reflection as a tensile wave, subsequently being transmitted back into the incident tube (as seen in Figure 3b). This transmission resulted in the detachment of the incident tube from the rigid mass, as illustrated in Figure 3c. The incident tube then impacted the transfer flange, which stopped the movement of the incident bar toward the specimen (Figure 3c). Consequently, the specimen only experienced a single load of known amplitude and duration. In the meantime, the impacts of the incident tube on the transfer flange created a reflected compressive wave that collided and superposed with the reflected tensile wave, which formed a resultant wave of lower amplitude (Figure 3c).

High-speed Camera

In order to verify whether the momentum trapping mechanism connected to the SHPB system is correct and reliable, high-speed real-time video pictures were needed. This analysis recorded the incident bar movement within five frames when the specimen was struck. The high-speed camera is synchronized manually with the first movement of the projectile to allow the camera to capture the whole deformation process.

A high-speed image sequence with a frame rate of about 5000 fps and higher was acquired during dynamic experiments. A strong light source at this speed was sufficient to minimize exposure time and obtain “frozen” images. Two light sources were used at the same frequency as the camera’s frame rate. The light exposure was checked to avoid thermal effects on the mechanical properties of the tested material. Figure 4 shows a high-speed camera and light source setup during the SHPB experiment.

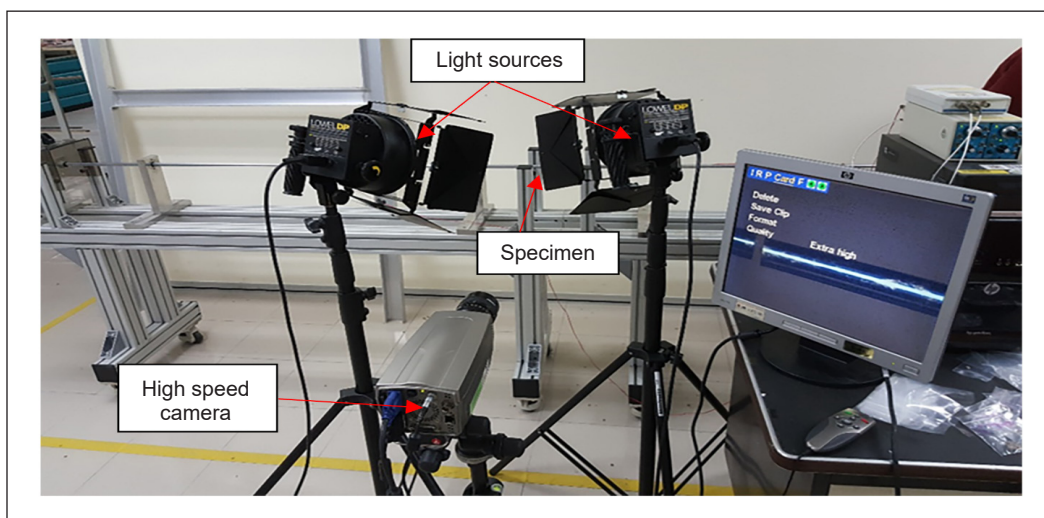


Figure 4. High speed camera setup during impact loading

Materials

Long unidirectional fiber yarns of tex 1400 used were supplied by JUTEKO Bangladesh, Pvt. Ltd. Bangladesh. The tex number of the yarn refers to the diameter size of the yarn used for the pultrusion process. Tex is defined as a unit of measurement for the linear mass density of fibers and the mass in grams per 1000 meters. Unsaturated polyester resin (Crystic P9901) was purchased from the Revertex Company, Malaysia. Other mixtures for resin, such as benzoyl peroxide (BPO) as initiator, calcium carbonate (CaCO_3) as filler and the release agent powder, were supplied by Revertex Company as well. A thermoset pultrusion machine model no. SVS-PUL-6T at the School of Materials and Mineral Resources Engineering, Universiti Sains Malaysia, produced the pultruded kenaf fiber reinforced composites samples. By using 55 kenaf yarns tex of 1400, a pultruded kenaf composite with 70% volume fractions (v/v %) has been produced, as shown in Figure 5. A pultruded kenaf composite with a diameter size of 12.7 mm that has been produced was then cut into 7 mm of length.



Figure 5. Kenaf composite specimen

RESULTS AND DISCUSSION

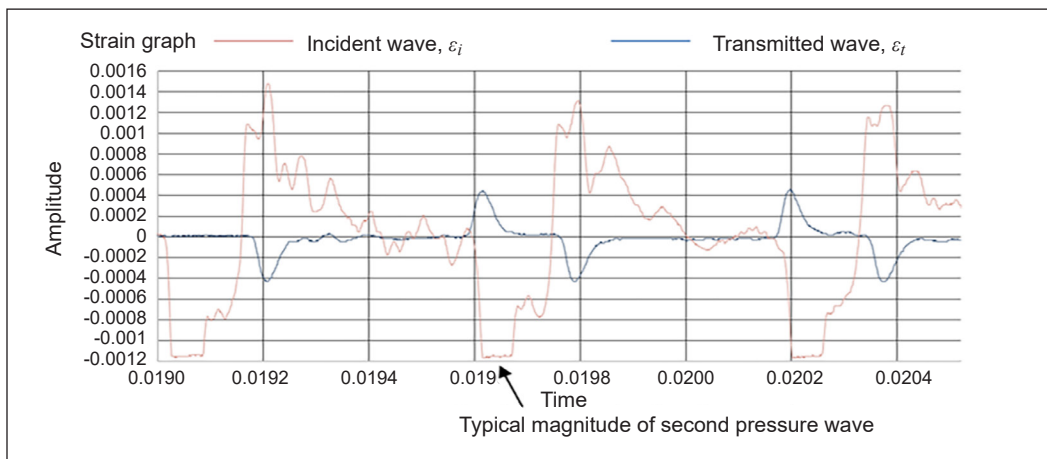
Figure 6 shows the example of two waves reported for experimentation in the Hopkinson bars without (a) and with (b) the momentum trap. In general, with and without a momentum trap, the incoming wavelength is similar to the minimal effect of the transfer flange. In an untrapped Split Hopkinson Pressure Bar, the incident bar hit the specimen several times, as shown in Figure 7a, where the second and third waves are held at a strain magnitude of 0.0012 at the time of 0.0196s and 0.0202s, respectively.

Contrariwise, the secondary wave of compression was decreased by 50 percent in the application of momentum trapping (refer to the difference in incident bar signals of around 0.0196 μs to 0.0198 μs). The second compression wave's changes in magnitude indicate that the tensile wave reflected in the input bar was disturbed by the wave induced by the impact of the flange tube. The remaining tensile wave was then reflected as the second compressive wave at the free end of the incident bar. Although the second compressive wave was not completely isolated or returned as a tensile wave, the effect of the incident tube on the flange was sufficient to ensure that the specimen was not in contact with the tube and, thus, was loaded only once. A similar result has also been reported by Xia and Yao (2015), where the second compressive wave has been reduced by implementing a momentum trapping system in SHPB.

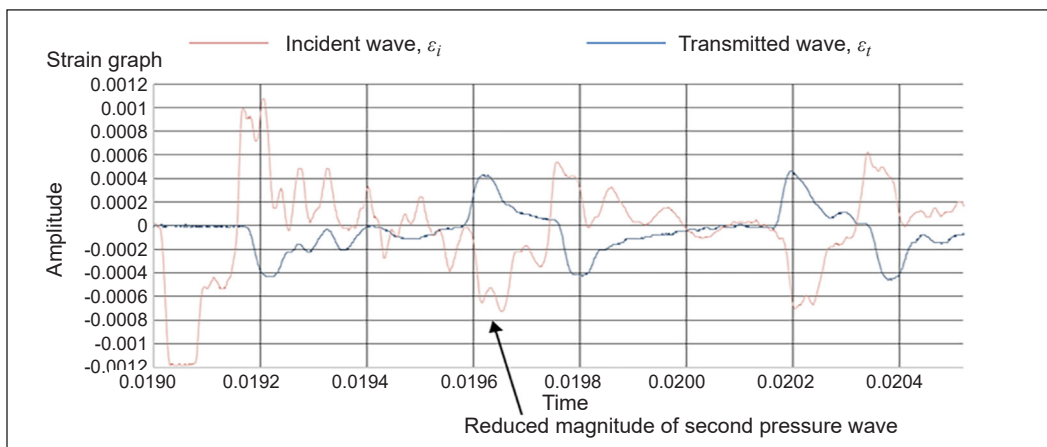
The data from the high-speed camera were utilized to distinguish between the condition of the specimen with and without the momentum trapping. In Figure 7a, from the time

of 0.0190s to 0.0198s, where the momentum trapping was excluded from the SHPB, the specimen was loaded four times, and the input bar moved further towards the specimen. This unnecessary movement of the incident bar has created additional damage to the specimen, as shown in Figure 9. However, as shown in Figure 7b from the time range of 0.0190s until 0.0198s, it is evident that, when using the momentum trapping, after the loading of the specimen at a time of 0.0192s, the output bar, which does not include a momentum trap, goes away while the input bar's face stays still. Therefore, it is established that the specimens experienced a single loading event.

An incident tube and a rigid mass were separated by a predetermined gap, as depicted in Figure 8a. After the incident tube has made contact with the rigid mass (Figure 8d), a secondary loading wave reflected in the incident bar will arrive and cause the gap



(a)



(b)

Figure 6. Strain-time history graphs in incident and transmitter bars (a) without momentum trap, and (b) with momentum trap

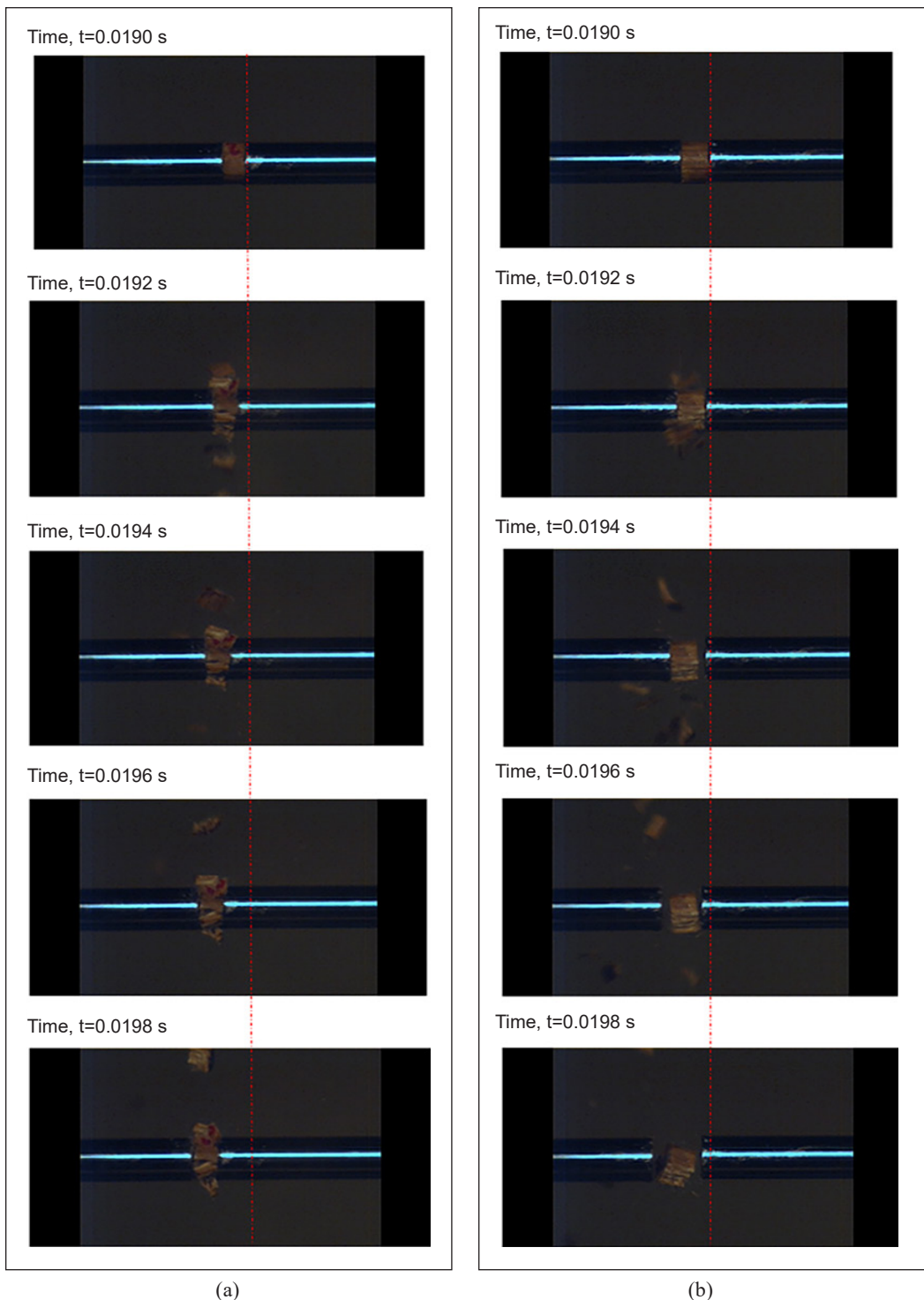


Figure 7. High speed images of specimen's condition during impact loading (a) without momentum trap (b) with momentum trap

between the incident tube and the transfer flange to close (Figure 8e). As the gap was closed (Figure 8d), a reverse compressive pulse resulted from the impact of the incident tube on the flange, causing the incident bar to stop abruptly. As the needless momentum was extracted to ensure a single load on the specimen, the state of the specimen was established by the defined load, and the development of damage within a specimen was easier to identify. The movement of the incident tube during the impact is shown in Figures 8a to 8e.

Proper care should be taken to establish the precise distance between the transfer flange and the stiff mass to achieve satisfactory results. To be precise, if the distance is too great, the effect of the incident tube on the transfer flange would not be sufficient to prevent further specimen loading by the incident bar. On the other hand, if the gap is too short, a reflected secondary load wave in the incident bar might arrive even at the incident tube position, and the flange is not closed. It may impact the stress pulse, shift the incident tube to an incorrect location, or do both, resulting in unwanted results.

Figure 9 shows the stress-strain curves of the kenaf composite under strain rates of 1000/s until 1400/s. As strain rates increased, both stiffness and compressive strength decreased. Reductions in both properties were relatable to the failure images of kenaf composite specimens (Figure 10), where specimens have endured

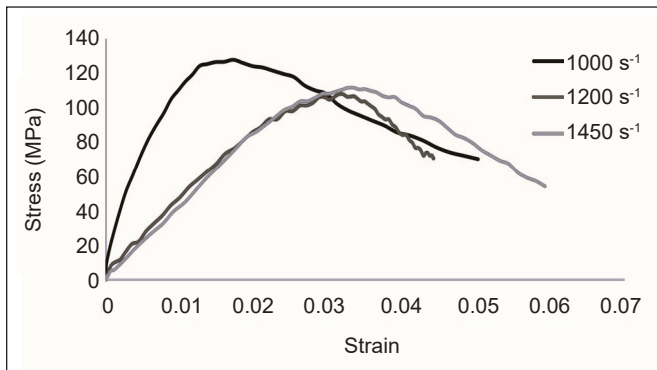
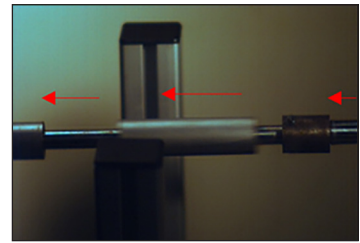


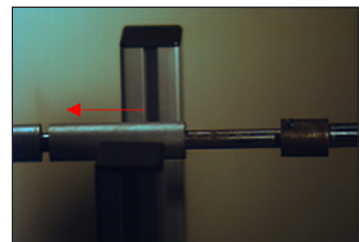
Figure 9. Compressive stress-strain curve of kenaf composite under different strain rates



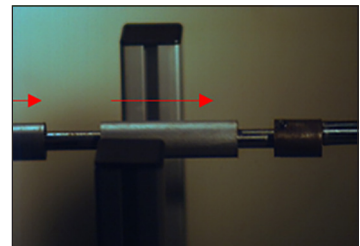
(a)



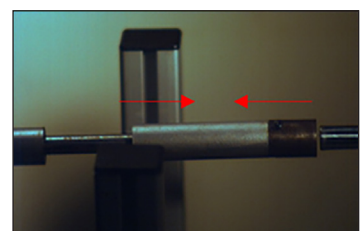
(b)



(c)



(d)



(e)

Figure 8. Sequence of movement of momentum trap during impact loading

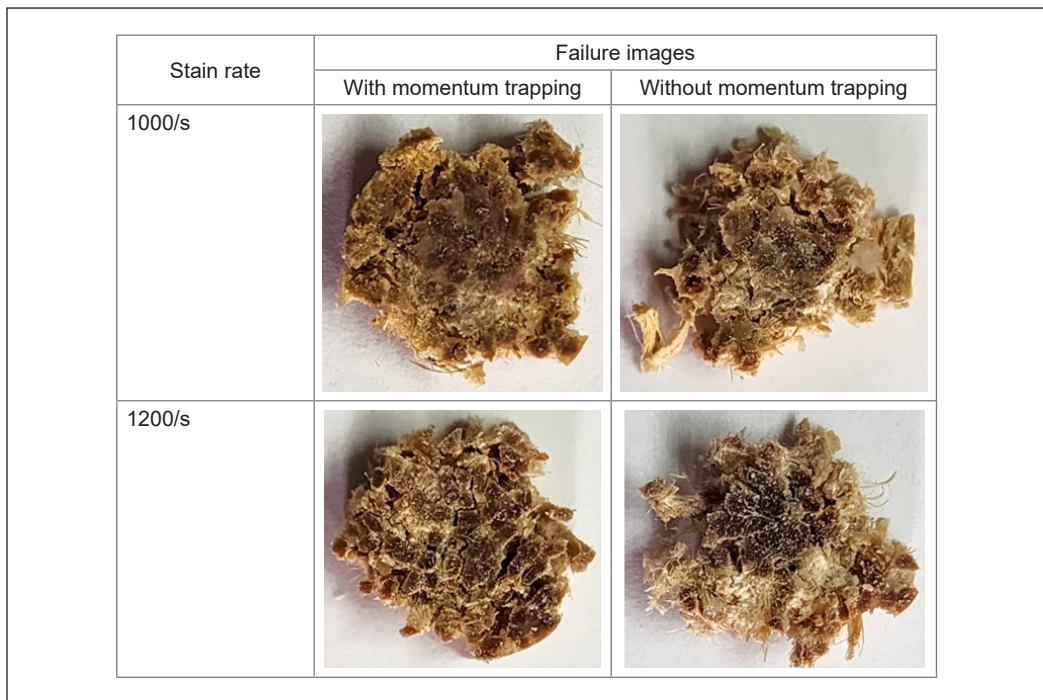


Figure 10. Failures of kenaf composite under different strain rates with and without momentum trapping

more extensive matrix cracking and fiber fracture damages as strain rates increased. According to Seman et al. (2019a), heat generated during impact has increased the molecular mobility of resin, which has contributed to a reduction in compressive properties and values.

The correlation between different strain rate levels and microstructural damages to a kenaf composite with and without momentum trapping is shown in Figure 10. Under strain rates of 1000/s and 1200/s, kenaf composite specimens have endured more catastrophic damages as the incident bar repeatedly impacted it when momentum trapping was not installed (Figure 7). Meanwhile, the installation of momentum trapping has helped to abstain from the secondary and subsequent movement of the incident bar toward the specimen, and less damage has been found on the specimen, as shown in Figure 10. By eliminating the repeated movement of the incident bar, unnecessary damage to specimens can be avoided. Thus, an exact correlation between different strain rate levels and microstructural damages to a kenaf composite can be made.

CONCLUSION

The classical split Hopkinson pressure bar and a unique and simple momentum trapping method for recovering dynamic specimens were introduced. The technique enables dynamic specimen recovery with a much smaller rigid mass and less complicated momentum trap

arrangement, thus facilitating the installation and commissioning of the test. An effective dynamic process has successfully realized the recovery of kenaf composite specimens through a single deformation event. This achievement is confirmed by the significant reduction of the secondary wave by approximately 50%, which stopped the repeated movement of the incident bar and additional damage to the specimens. Therefore, an exact correlation between different stress rate levels and microstructural damages to kenaf composites has been obtained.

ACKNOWLEDGEMENT

The authors would like to thank the Ministry of Higher Education, Malaysia, under the Fundamental Research Grant Scheme (FRGS) ref: FRGS/1/2023/STG05/USM/03/1 and Universiti Sains Malaysia Short Term Grant 304/PMEKANIK/6315493 for supporting this research.

REFERENCES

- Abidin, N. M. Z., Sultan, M. T. H., Shah, A. U. M., Shahar, F. S., Najeeb, M. I., Ali, M. R., Basri, A. A., Baloor, S. S., Gaff, M., & Hui, D. (2023). The evaluation of the mechanical properties of glass, kenaf, and honeycomb fiber-reinforced composite. *Reviews on Advanced Materials Science*, 62(1), Article 20220299. <https://doi.org/10.1515/rams-2022-0299>
- Alshammari, M. B., Ahmad, A., Jawaid, M., & Awad, S. A. (2023). Thermal and dynamic performance of kenaf/washingtonia fibre-based hybrid composites. *Journal of Materials Research and Technology*, 25, 1642-1648. <https://doi.org/10.1016/j.jmrt.2023.06.035>
- Arjmandi, R., Yıldırım, I., Hatton, F., Hassan, A., Jefferies, C., Mohamad, Z., & Othman, N. (2021). Kenaf fibers reinforced unsaturated polyester composites: A review. *Journal of Engineered Fibers and Fabrics*, 16, Article 15589250211040184. <https://doi.org/10.1177/15589250211040184>
- Arockia Dhanraj, J., G, D., Kumar, S., Sivakumar, S., & Vishnuvardhan, R. (2019). *Experimental investigation on mechanical properties and vibration damping frequency factor of kenaf fiber reinforced epoxy composite*. SAE Technical Papers, 2019-28-0167. <https://doi.org/10.4271/2019-28-0167>
- Bhambure, S. S., Rao, A. S., & Senthilkumar, T. (2023). Analysis of mechanical properties of kenaf and kapok fiber reinforced hybrid polyester composite. *Journal of Natural Fibers*, 20(1), Article 2156964. <https://doi.org/10.1080/15440478.2022.2156964>
- Holbery, J., & Houston, D. (2006). Natural-fiber-reinforced polymer composites in automotive applications. *The Journal of The Minerals, Metals & Materials Society*, 58, 80-86. <https://doi.org/10.1007/s11837-006-0234-2>
- Mansingh, B. B., Binoj, J. S., Manikandan, N., Sai, N. P., Siengchin, S., Rangappa, S. M., Bharath, K. N., & Indran, S. (2022). Chapter 12 - Kenaf fibers, their composites and applications. In S. M. Rangappa, J. Parameswaranpillai, S. Siengchin, T. Ozbakkaloglu, & H. Wang (Eds.), *Plant Fibers, Their Composites, and Applications* (pp. 283-304). Woodhead Publishing. <https://doi.org/10.1016/B978-0-12-824528-6.00011-4>

- Millogo, Y., Aubert, J. E., Hamard, E., & Morel, J. C. (2015). How properties of kenaf fibers from Burkina Faso contribute to the reinforcement of earth blocks. *Materials*, 8(5), 2332-2345. <https://www.mdpi.com/1996-1944/8/5/2332>
- Nemat-Nasser, S., Isaacs, J. B., & Starrett, J. E. (1991). Hopkinson Techniques for dynamic recovery experiments. *Proceedings: Mathematical and Physical Sciences*, 435(1894), 371-391. <http://www.jstor.org/stable/51971>
- Ochi, S. (2008). Mechanical properties of kenaf fibers and kenaf/PLA composites. *Mechanics of Materials*, 40(4-5), 446-452. <https://doi.org/https://doi.org/10.1016/j.mechmat.2007.10.006>
- Omar, M. F., Akil, H. M., Ahmad, Z. A., Mazuki, A. A. M., & Yokoyama, T. (2010). Dynamic properties of pultruded natural fibre reinforced composites using split Hopkinson pressure bar technique. *Materials & Design*, 31(9), 4209-4218. <https://doi.org/https://doi.org/10.1016/j.matdes.2010.04.036>
- Prot, M., & Cloete, T. J. (2016). A tandem momentum trap for dynamic specimen recovery during split Hopkinson pressure bar testing of cancellous bone. *Journal of Dynamic Behavior of Materials*, 2, 50-58. <https://doi.org/10.1007/s40870-016-0046-6>
- Saba, N., Paridah, M. T., & Jawaid, M. (2015). Mechanical properties of kenaf fibre reinforced polymer composite: A review. *Construction and Building Materials*, 76, 87-96. <https://doi.org/https://doi.org/10.1016/j.conbuildmat.2014.11.043>
- Seman, S. A. H. A., Ahmad, R., & Akil, H. M. (2019a). Experimental and numerical investigations of kenaf natural fiber reinforced composite subjected to impact loading. *Polymer Composites*, 40(3), 909-915. <https://doi.org/10.1002/pc.24758>
- Seman, S. A. H. A., Ahmad, R., & Akil, H. M. (2019b). Meso-scale modelling and failure analysis of kenaf fiber reinforced composites under high strain rate compression loading. *Composites Part B: Engineering*, 163, 403-412. <https://doi.org/10.1016/j.compositesb.2019.01.037>
- Sharba, M., Salman, S., Leman, Z., Sultan, M., Ishak, M., & Hanim, M. (2016). Effects of processing method, moisture content, and resin system on physical and mechanical properties of woven kenaf plant fiber composites. *Bioresources*, 11(1), 1466-1476.
- Song, B., & Chen, W. (2004). Loading and unloading split Hopkinson pressure bar pulse-shaping techniques for dynamic hysteretic loops. *Experimental Mechanics*, 44, 622-627. <https://doi.org/10.1007/BF02428252>
- Tamrakar, S., Kiziltas, A., Mielewski, D., & Zander, R. (2021). Characterization of kenaf and glass fiber reinforced hybrid composites for underbody shield applications. *Composites Part B: Engineering*, 216, Article 108805. <https://doi.org/https://doi.org/10.1016/j.compositesb.2021.108805>
- Uzoma, A. E., Nwaeche, C. F., Al-Amin, M., Muniru, O. S., Olatunji, O., & Nzeh, S. O. (2023). Development of interior and exterior automotive plastics parts using kenaf fiber reinforced polymer composite. *Eng*, 4(2), 1698-1710. <https://www.mdpi.com/2673-4117/4/2/96>
- Vasilash, G. S. (2020). *Natural fiber-reinforced composite developed for Toyota EV concept*. Gardner Business Media. <https://www.gardnerweb.com/articles/natural-fiber-reinforced-composite-developed-for-toyota-ev-concept>

- Wazeer, A., Das, A., Abeykoon, C., Sinha, A., & Karmakar, A. (2023). Composites for electric vehicles and automotive sector: A review. *Green Energy and Intelligent Transportation*, 2(1), Article 100043. <https://doi.org/https://doi.org/10.1016/j.geits.2022.100043>
- Xia, K., & Yao, W. (2015). Dynamic rock tests using split Hopkinson (Kolsky) bar system – A review. *Journal of Rock Mechanics and Geotechnical Engineering*, 7(1), 27-59. <https://doi.org/https://doi.org/10.1016/j.jrmge.2014.07.008>
- Zhang, K., Sun, Y., Wang, F., Liang, W., & Wang, Z. (2020). Progressive failure and energy absorption of chopped bamboo fiber reinforced polybenzoxazine composite under impact loadings. *Polymers*, 12(8), Article 1809. <https://doi.org/10.3390/polym12081809>